Available online at www.sciencedirect.com

ScienceDirect

journal homepage: www.elsevier.com/locate/he

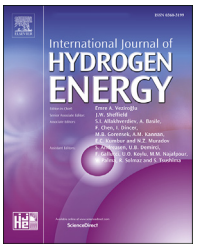

Flame structure, turbulent burning velocity and its unified scaling for lean syngas/air turbulent expanding flames

Haoran Zhao, Jinhua Wang, Xiao Cai, Hongchao Dai, Zhijian Bian, Zuohua Huang*

State Key Laboratory of Multiphase Flow in Power Engineering, Xi'an Jiaotong University, Xi'an, 710049, China

HIGHLIGHTS

- Turbulent expanding flames of syngas/air are investigated up to 80% H_2 fraction.
- The effects of H_2 fraction on S_T are interpreted in detail.
- A unified scaling of S_T is obtained using Re_T when *Le* is close to unity.
- Turbulent expanding flames follow a self-similar propagation and $S_T \sim R^{0.5}$ approximately.

ARTICLE INFO

Article history:
Received 15 August 2020
Received in revised form
15 April 2021
Accepted 12 May 2021
Available online 10 June 2021

Keywords:
Turbulent burning velocity
Syngas
High hydrogen fraction
Unified scaling
Turbulent expanding flames

ABSTRACT

A systematic experimental study of lean premixed syngas/air turbulent expanding flames has been conducted under a wide range of turbulence intensities (0–3.54 m/s), initial pressures (0.5–5 bar), and hydrogen volumetric fractions up to 80% (20%, 50% and 80%). Flame structure and turbulent flame propagation dynamics were investigated. Results show that the flame becomes more refined and wrinkled with the increasing of both turbulence intensity and initial pressure, leading to a larger flame area and the associated turbulent burning velocity (S_T). With hydrogen fraction increased, S_T is also enhanced significantly, which is mainly due to the promotion of laminar burning velocity (S_L) and diffusional-thermal instability. S_T/S_L is nearly kept constant with hydrogen fraction, which is a trade-off between strengthened diffusional-thermal instability and weakened turbulence stretch. A unified scaling of S_T is obtained, indicating that turbulent Reynolds number (Re_T) is a practical method to correlate S_T when Lewis number is close to unity. Furthermore, at least in the interpretation domain, S_T of spherical flames continually increases as the flame expands, which has been referred as flame acceleration phenomenon. It appears that only effective turbulence intensity itself is not able to reflect acceleration phenomenon completely. Turbulent expanding flames follow a self-similar propagation law and the quantitative S_T dependence with flame expanding is $S_T \sim R^{0.5}$ approximately.

* *Corresponding author.*
E-mail address: jinhuawang@mail.xjtu.edu.cn (J. Wang).

https://doi.org/10.1016/j.ijhydene.2021.05.090

Introduction

Hydrogen enriched fuels have many benefits, such as improving the flammability limits, enhancing the burning velocity and reducing the CO_2 emission [1]. Syngas is a typical hydrogen enriched fuel with the main composition of CO and H_2, which has diversity feedstocks such as Integrated Gasification Combined Cycle (IGCC) [2], and it is also a potential fuel for gas turbine, internal combustion engines and industry burners [3,4]. There is a large variation of hydrogen fractions in syngas due to the different feedstocks as well as gasification technique, which has significant effects on combustion stability and thus combustor design and operation. Furthermore, fuel lean premixed combustion can increase the thermal efficiency and significantly reduce the NOx and soot emissions [5]. However, the flame characteristics of hydrogen enriched fuels can be affected a lot by initial conditions, such as hydrogen fraction, initial pressure (P) and so on. Considering that turbulent flame is more conventional in practical application, turbulence intensity (u') will also play an important role and be coupled with other factors. Thus, it is necessary to conduct a systematic study of lean premixed syngas/air turbulent flames and investigate the effects of these factors on flame propagation dynamics, especially turbulence intensity and hydrogen fraction.

Turbulent combustion chamber is a classical experimental apparatus to investigate the interactions between turbulence and flame, mainly concentrating on turbulent expanding flames [6,7]. Compared with stationary flame configurations such as Bunsen burner, turbulent combustion chamber could provide an intense and isotropic turbulence environment more easily by adjusting the fan rotational speed [8,9]. At the same time, the turbulence field is more uniform due to a less effect of boundary layer. Also, it can achieve a high pressure condition more safely and economically. Because of these benefits, many experiments have been conducted through turbulent combustion chamber [10–16], and the most important parameter is turbulent burning velocity.

Turbulent burning velocity is important for practical combustor design and modification, which reflects the burning intensity and fuel consumption rate. Thus, it has been determined using combustion chamber under a wide range of conditions, especially for individual fuel, such as hydrogen [12,17–19], methane [20–25], isooctane [11,26,27] and alcohols [28,29]. Comparatively, for hydrogen blending binary fuel, relative studies especially for turbulent expanding flames are not enough. Mandilas et al. [30] investigated the effects of 5% hydrogen addition on methane and isooctane turbulent expanding flames at 5 bar, finding that hydrogen addition could improve turbulent burning velocity effectively, and the improvement was more evident at fuel-lean side but gradually weakened with the increasing equivalence ratio (φ). Fairweather et al. [20] measured the turbulent burning velocity of methane/hydrogen turbulent expanding flames with different hydrogen fractions (10%, 20% and 50%) at atmosphere and 360 K, concluding that hydrogen addition could reduce Markstein number and increase turbulent burning velocity, and this increase would be more strengthened in intense turbulence. Muppala et al. [31] obtained the turbulent burning velocity of methane/hydrogen and propane/hydrogen flames, and used them to test an algebraic flame surface wrinkling reaction model through mean local burning velocity and critical chemical time scale. Results showed that both approaches could have a qualitative prediction. Cai et al. [32] investigated the self-similar propagation of methane/hydrogen turbulent expending flames under different hydrogen fractions (20%, 50% and 80%) and validated that the molecule diffusion had significant effects on turbulent flame propagation even in intense turbulence. Shy et al. [13,33] measured the turbulent burning velocity of syngas with 35% hydrogen fraction from 1 to 10 bar and it appeared that turbulent burning velocity increased with initial pressure when turbulent Reynolds number (Re_T) was not controlled. But when turbulent Reynolds number was kept constant, turbulent burning velocity decreased with initial pressure, which was consistent with laminar flame speed (S_L). Jiang et al. [34] studies the effects of hydrogen fraction on syngas combustion characteristics under atmospheric temperature and pressure, and found the promotion of turbulence on burning velocity decreased gradually when hydrogen fraction was more than 50%. Zhang et al. [35] investigated the acceleration characteristics of syngas with 10% hydrogen fraction, indicating that the acceleration exponent and fractal excess of turbulent premixed flames decreased with equivalence ratio and increased with turbulence intensity. Sun et al. [36,37] investigated the stoichiometric syngas/air turbulent expanding flames up to 90% hydrogen fraction and proposed the empirical correlations of explosion characteristics and turbulent burning velocity. Most previous researches concentrated on methane/hydrogen flames, and only a few of them investigated syngas. Meanwhile, most hydrogen fractions were no more than 50%, and higher fraction (80%) is limited. Furthermore, all above experimental data were conducted at atmosphere and elevated pressures, and none of them came down to sub-atmosphere condition. As we know, sub-atmosphere condition is very important in some practical applications such as aircraft engines at high altitude. Thus, it is necessary to extend the turbulent burning velocity of syngas in wide conditions.

In addition, the unified scaling of turbulent burning velocity is also very important for combustor design and operation, and it can be utilized as a closure parameter in many turbulent premixed flame modelling approaches, such as Flame Surface Density (FSD) [38], Turbulent Flame speed Closure (TFC) [39] and G-equations [40]. Kitagawa et al. [12] considered the effects of molecular transport and tried to obtain a unified scaling through Lewis number (*Le*) and turbulent Reynolds number, but the correlation was quantitatively different in wide turbulent intensity ranges. Chaudhuri et al. [41] used the spectral closure of G-equation and derived that turbulent burning velocity was proportional to the square root of turbulent Reynolds number, which was mainly suitable for $Le \approx 1$ condition. Also, the effects of hydrodynamic instability were not considered in this correlation. Liu et al. [23] correlated turbulent burning velocity with turbulent Reynolds number and validated that a power law was suitable with a factor of 0.53, which is near to the previous theoretical result. Also, they transferred the experimental data into progress variable $\bar{c} \approx 0.5$ and obtained a satisfactory correlation through Kobayashi model [42], Zimont model [43] and DRZ model [44]. Many mathematical models have been proposed in a variety of

forms, and some of these models were able to achieve a genera correlation of turbulent burning velocity under certain conditions [43]. However, most models only concentrated on global turbulent burning velocity, a specific value under a certain condition, but ignored the acceleration phenomenon during the flame propagating outwardly.

For turbulent expanding flames, transient turbulent burning velocity will gradually grow up with flame radius (R), and a satisfactory formulation should also take this meaningful and interesting phenomenon into account. In order to analyze and explain this phenomenon, Abdel-Gayed and Bradley et al. [45] point out that the flame could only be wrinkled by eddies smaller than itself while larger eddies could only have a convective effect. Thus, the concept of effective turbulence intensity (u'_{eff}), and its estimation methods were proposed, which stands for a constantly changing turbulence intensity with flame propagating outwardly. Except for that, Chaudhuri et al. [9] chose another way and directly replaced integral length scale (L_T) by flame radius in turbulent Reynolds number, which achieved a reasonable unified scaling of turbulent burning velocity. Although turbulent flame acceleration has been investigated by some experiments [18,19,32,46,47], it is still an open issue. Until now, the ability of effective turbulence intensity still needs to be validated. In other words, corresponding to the unified scaling, if the introduction of effective turbulence intensity is enough to reflect the acceleration phenomenon in turbulent expanding flames is unknown. The flame radius itself seems to be able to reflect this acceleration phenomenon, while a quantitative description of this dependence also needs to be clarified. Besides, a better general correlation is still worth looking forward to, when effective turbulence intensity and flame radius are introduced together.

The objective of this study is to investigate the flame propagation dynamics of syngas/air turbulent premixed flames. The systematic experiments of lean syngas/air turbulent expanding flames were conducted in our newly developed turbulent combustion chamber over a wide range of conditions. Firstly, turbulent burning velocity is determined under different turbulence intensities and initial pressures, including sub-atmosphere, to extend the existing experimental data of syngas. Also, their effects on flame structure and turbulent burning velocity are analyzed and validated. Secondly, turbulent burning velocity is compared under 20%, 50% and 80% hydrogen volumetric fractions. During this process, a detailed and comprehensive analysis is conducted to clarify the influencing mechanism of hydrogen addition. Finally, a unified scaling of turbulent burning velocity is derived, in consideration of acceleration phenomenon or not, respectively. Especially, the quantitative description of acceleration phenomenon and the capability of effective turbulence intensity will be analyzed in detail.

Experimental setup and procedures

Turbulent combustion chamber

The experiments were conducted on a newly developed spark-ignition, constant volume, fan-stirred turbulent combustion chamber as show in Fig. 1. And the detailed information of this chamber can be referred in Ref. [48]. The volume is 22.6 L, with a 305 mm inner diameter and 310 mm inner length. Two quartz windows are equipped on both sides of the chamber, with an optical diameter of 150 mm allowing for schlieren or shadow imaging. Four impellers are mounted in diagonal positions which are coupled to electric motors with independent speed controllers, and the maximum speed of motors can be up to 10,000 rpm. Two electrodes are located on chamber wall symmetrically for the ignition of gas mixture. A heating wall is embedded in chamber to heat gas mixture to the target temperature, which is monitored by an Omega thermocouple. Two pressure transmitters are mounted to the chamber, used for the monitoring of introduced gas pressure (Rosemount) and transient explosion pressure (Kistler 6125C), respectively. All turbulent spherically expanding flames are captured by shadow imaging through a high-speed digital camera (Phantom v611). It is worth pointing out that the turbulent combustion chamber is a high-pressure high-temperature vessel, whose maximum initial pressure and temperature can be up to 10 bar and 473 K, respectively. And except for high pressures, the spherically expanding flames can also be measured under sub-atmospheric pressure because of its good vacuum and efficient ignition system.

Data processing procedures

Due to that turbulent expanding flames are not so regular as laminar conditions, the flame radius is obtained through area method. That is, the flame front is fitted with a circle of equal area (A), then the flame radius is estimated by $R=(A/\pi)^{0.5}$. After that, a differential dR/dt is conducted between flame radius and time, and that is flame propagation speed. Divided by thermal expansion ratio (σ), the transient turbulent burning velocity ($S_{T,R}$) corresponding to unburned gas mixture is obtained in final. The flame radius range of 10–45 mm is selected to estimate turbulent burning velocity, in order to eliminate the disturbance of ignition and chamber confinement [49,50]. To compare with stationary flame results and validate relative models, an individual value of turbulent burning velocity should be ensured corresponding to an individual condition. Due to the acceleration of turbulent expanding flames, it is difficult to determine a specific value. For this, various methods have appeared in literatures of different groups

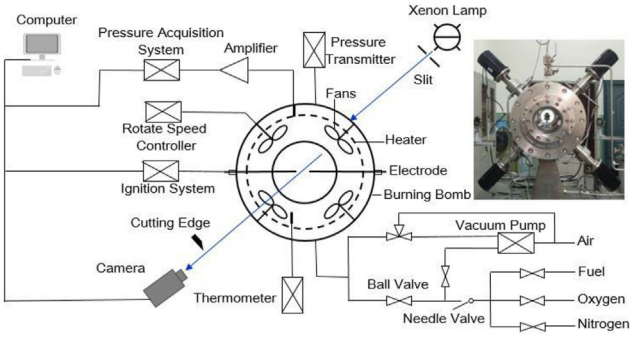

Fig. 1 – The schematic of fan-stirred turbulent combustion chamber.

[23,26,46]. In current study, an average process is conducted to transient turbulent burning velocity in the selected flame radius range, and then the individual value is obtained, which can be called global turbulent burning velocity (S_T) here. According to the study of Bradley et al. [28], turbulent burning velocity determined by schlieren or shadow radius corresponds to the progress variable $\bar{c}\approx 0.1$. And it can be transferred into other reference radius through the methods in literature [8,28].

Experimental conditions

Syngas/air turbulent expanding flames are obtained through a combustion chamber, and the detailed experimental conditions are shown in Table 1. The hydrogen volumetric fraction in syngas is 20%, 50% and 80%, respectively. And the initial pressure range is 0.5–5 bar. Turbulence intensity u' is indicated by root mean square (RMS) of velocity fluctuation, which is changed from 0 to 3.54 m/s through adjusting fan rotational speed (ω), to investigate its effects independently. According to the previous turbulence measurement [48], turbulence intensity and integral length scale are independent on ambient pressure and can be estimated by $u'\approx 1.77\cdot 10^{-3}\cdot\omega$ and $L_T\sim 0.719\cdot\omega^{0.376}$, respectively. All experiments are conducted at fuel lean conditions of $\varphi = 0.7$ and ambient temperature approximately 298 K. For turbulent expanding flames, 5 consecutive loops are carried out for each condition, while 3 loops are chosen for laminar flames. All experimental conditions are distributed in the flamelet zone and thin reaction zone as described in the classical premixed turbulent combustion regime diagram [51] in Fig. 2, indicating that turbulence eddies are not able to enter into the flame reaction zone. Thus, the flame itself can be treated as laminar flamelet, and turbulence mainly causes stretch and wrinkled effects on it.

Results and discussions

Effects of turbulence intensity and initial pressure

The spherically expanding flames of lean syngas/air are obtained through shadow imaging method, which are shown in Fig. 3 (a) and (b). According to the turbulence characteristics estimation [48], Kolmogorov length scale will be decreased with turbulence intensity and initial pressure, which indicates the smallest length scale of turbulence field will be extended to a lower value. As a result, the flame geometry will become more refined and wrinkled with the increasing of turbulence

Table 1 – Experimental conditions in this study.

Syngas	φ	T (K)	P (bar)	u' (m/s)
$CO/H_2 = 80/20$	0.7	298	1	0, 0.89, 1.77, 2.66, 3.54
			0.5, 1.5, 2, 2.5, 3, 3.5, 5	1.77
$CO/H_2 = 50/50$			1	0, 0.89, 1.77, 2.66, 3.54
$CO/H_2 = 20/80$			1	0, 0.89, 1.77, 2.66, 3.54

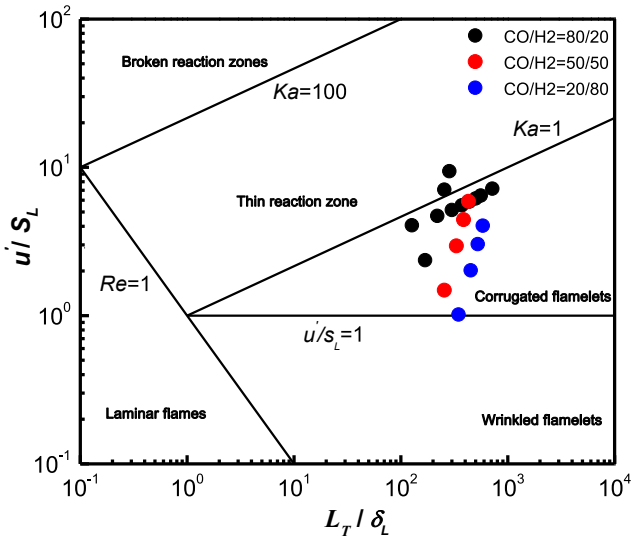

Fig. 2 – Turbulent premixed combustion regime diagram.

intensity and initial pressure, leading to a larger flame surface area. And the flame propagates to the same size with a shorter time, indicating a quicker flame propagation speed. Except that, with turbulence intensity increased, flame geometry becomes more irregular and reveals a stronger randomness. With initial pressure increased, the boundaries of flame gradually become more obvious, mainly due to a thinner flame thickness and sharper density gradient.

In order to analyze flame structure in a quantitative level, the wrinkling ratios are counted here. According to the study of Renou et al. [52], wrinkling ratio can be estimated as

$$w = R_p^2 \Big/ R^2 \tag{1}$$

where R and R_P is flame radius equal to burned gas area and perimeter, respectively. Fig. 4 shows the wrinkling ratios under different turbulence intensities and initial pressures. From Fig. 4 (a), we can see that wrinkling ratios are increased with turbulence intensity, indicating that flame becomes more wrinkled, which is consistent with the captured flame structure. It is also evident that wrinkling ratios will grow up with flame radius, although the distribution is more scattered in stronger turbulence. However, under different initial pressures, the wrinkling ratios don't appear an expected trend, as shown in Fig. 4 (b). Although wrinkling ratios still increase with flame radius, they seem to be disordered with initial pressure, which is inconformity with the intuitive vision of shadow images. For this contradiction, the possible reason may attribute to the limitation of shadow images and MATLAB codes. As initial pressure increases, the flame will be more refined and the small eddies have a more important effect than before. However, the resolution limitation may cause errors to image processing codes, thus the fine structures of flame can't be captured sometimes, leading to a larger uncertainty.

Fig. 5 is the transient turbulent burning velocity under different turbulence intensities and initial pressures. According to the classical theory of Damkohler [43], the growth of turbulent burning velocity is mainly caused by the larger flame area. Turbulence eddies can stretch the flamelets and wrinkle the

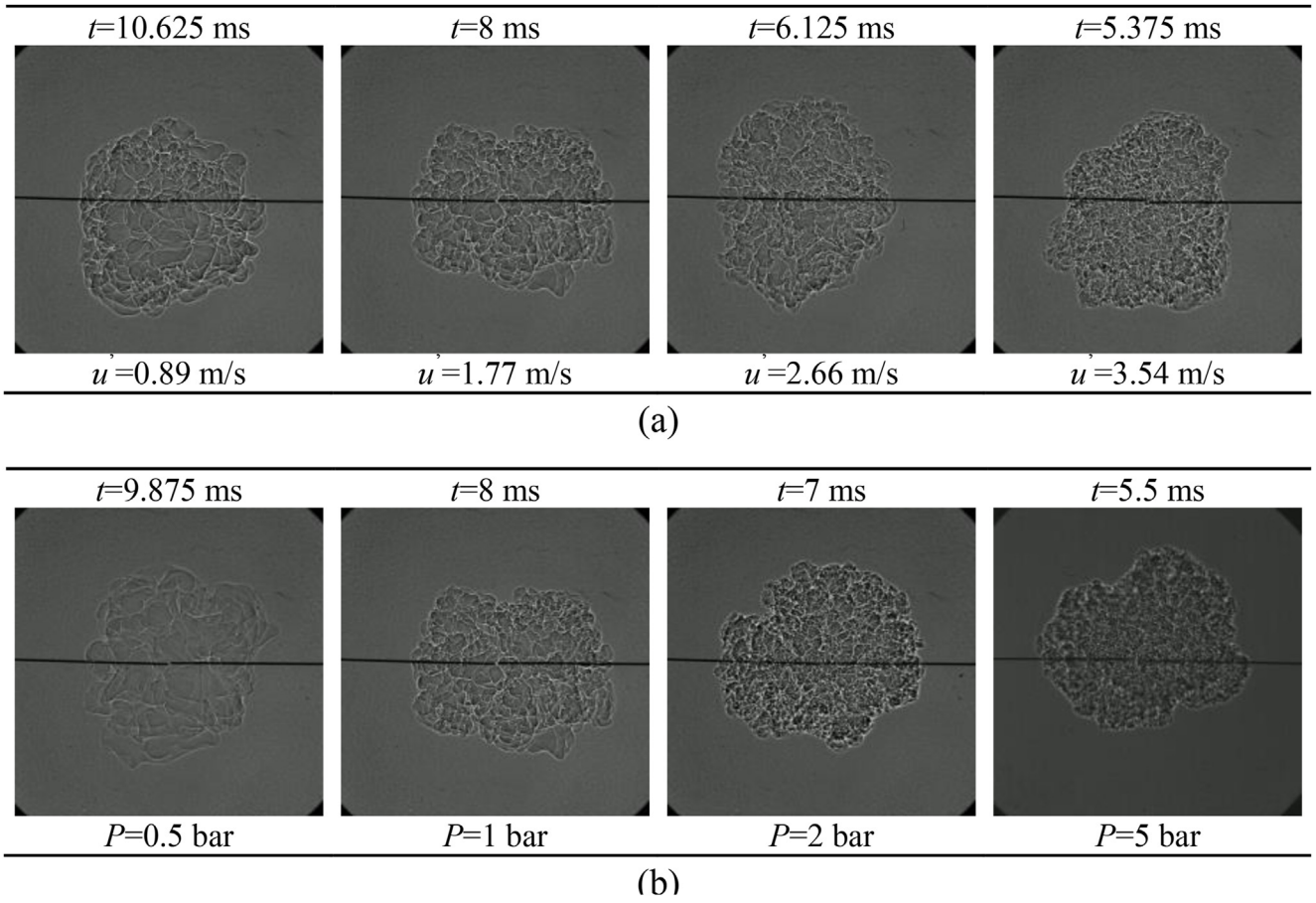

Fig. 3 – Flame morphology of syngas/air mixtures (CO/H_2 = 80/20) at R = 35 mm: (a) P = 1 bar under different u'; (b) u' = 1.77 m/s under different P.

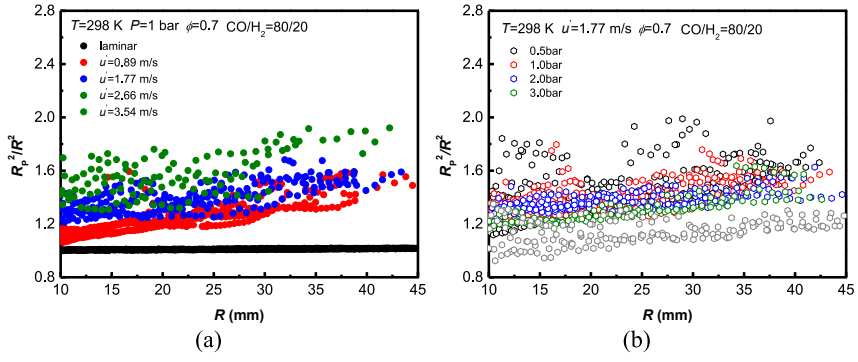

Fig. 4 – Wrinkling ratios under different conditions: (a) P = 1 bar under different u'; (b) u' = 1.77 m/s under different P.

flame surface. As turbulence intensity increased, the effects of turbulence stretch become strengthened, and the wrinkled degree of flamelets deepens accordingly. As a result, the flame area will be increased, contributing to a larger turbulent burning velocity. At the same time, the scatter of experimental data is also increased with turbulence intensity, which is mainly due to the randomness of turbulence itself. Thus, it is necessary to increase experimental loops corresponding to the intense turbulence condition. Similarly, as initial pressure increased, turbulent burning velocity will also have a growth trend, which is contrary to that of laminar burning velocity. It is known to us that flame is not only stretched by turbulence, but also affected by intrinsic instability, such as thermal-diffusional instability and hydrodynamic instability. On the one hand, flame thickness decreases with initial pressure, leading to a strengthened effect of hydrodynamic instability. More importantly, the turbulence itself will be varied. Although turbulence intensity is kept constant, other parameters of turbulence are affected by initial pressure. With initial pressure increased, Kolmogorov length scale (η) becomes smaller while turbulent Reynolds number has an evident growth, indicating that the stretch of turbulence vortex is strengthened at this

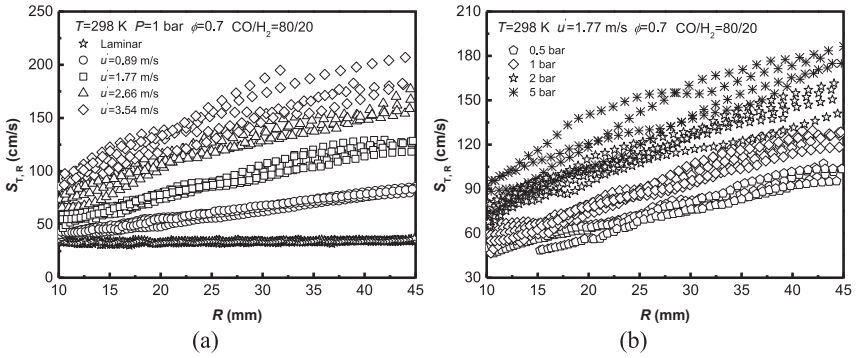

Fig. 5 – Transient turbulent burning velocity: (a) $P = 1$ bar under different u'; (b) $u' = 1.77$ m/s under different P.

time. Combining these two factors, flame area will become larger, leading to a larger turbulent burning velocity as well. Besides, it should be noted that all transient turbulent burning velocity is increased with flame radius, appearing a specific acceleration phenomenon.

Fig. 6 is the global turbulent burning velocity under different turbulence intensities and initial pressures, and the error bar is standard deviation of five loops. Similar to the transient value, global turbulent burning velocity is increased with turbulence intensity and initial pressure. Specifically, global turbulent burning velocity approximately performs a linear relation with turbulence intensity in current experimental range. But in fact, it will not be increased all the time. When turbulence intensity arrives at a critical value, global turbulent burning velocity will also reach its peak, and then come down with further increased turbulence intensity due to local extinction [53]. However, in current experimental conditions, there is no sign of local extinction, so global turbulent burning velocity is always increased. Except for that, it clearly indicates that global turbulent burning velocity is also increased with initial pressure, and the growth rate gradually becomes slow at high pressure, approximately following power law relation. As discussed above, this phenomenon can be interpreted by laminar flame thickness (δ_L) and Kolmogorov length scale. Fig. 7 is the laminar flame thickness and Kolmogorov length scale results, which correspond to the conditions in Fig. 6 (b). Here, laminar flame thickness is estimated by $\delta_L = \frac{\mu}{\rho S_L}$, where μ and ρ is dynamic viscosity and density of gas mixture, respectively. And the details about Kolmogorov

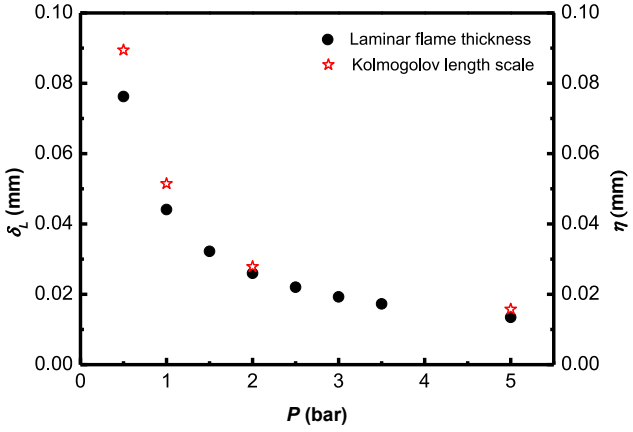

Fig. 7 – Laminar flame thickness and Kolmogorov length scale.

length scale can be found in Ref. [48]. It is obvious that both laminar flame thickness and Kolmogorov length scale decrease with initial pressure. And with initial pressure increasing, the variation trend will become smooth. As a result, the growth rate of turbulent burning velocity at high pressure will also become slow.

Effects of hydrogen fraction up to 80%

Fig. 8 is the transient turbulent burning velocity under different hydrogen fractions. The transient turbulent burning velocity is

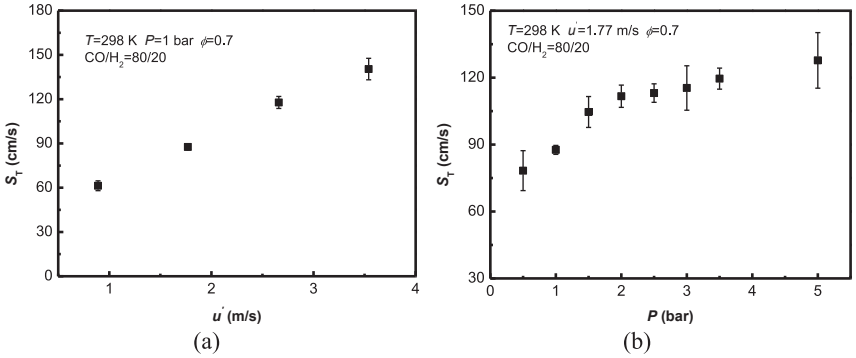

Fig. 6 – Global turbulent burning velocity: (a) $P = 1$ bar under different u'; (b) $u' = 1.77$ m/s under different P.

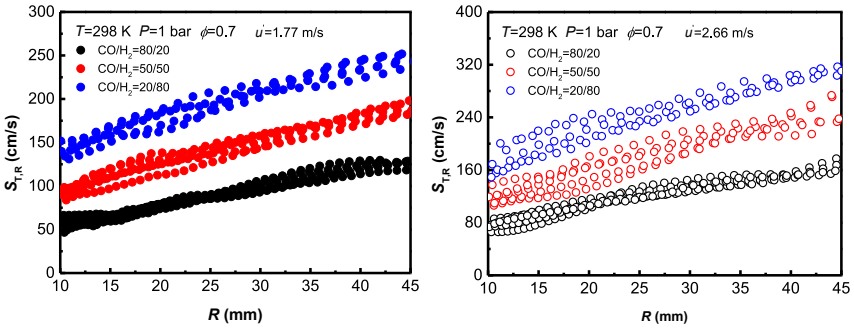

Fig. 8 – Transient turbulent burning velocity under different hydrogen fractions: (a) $u' = 1.77$ m/s; (b) $u' = 2.66$ m/s.

increased with hydrogen fraction, which is similar to that of laminar condition. Turbulent burning velocity is mainly dependent on turbulence and laminar flame properties. And the promotion of turbulent burning velocity can be interpreted by hydrogen fraction effects on laminar flame properties and molecular transport here. On the one hand, with hydrogen faction increased, the corresponding laminar burning velocity will also be increased, which will promote turbulent burning velocity. On the other hand, the diffusion rate of hydrogen is faster than others due to its small molecule. Thus, with hydrogen fraction increased, the ability of non-equal diffusion will be strengthened, which leads to a strengthened diffusional-thermal instability. Because of that, the flamelets will be more wrinkled and its turbulent burning velocity will become larger. Besides, flame thickness will also be reduced with the growth of hydrogen fraction, enhancing the effects of hydrodynamic instability as well. All relative parameters are calculated and shown in Table 2. It should be noted that syngas is a binary fuel, and Lewis number of syngas is evaluated through volume based formulation proposed by Muppala et al. [31]: $Le = x_1 Le_{CO} + x_2 Le_{H_2}$. Here, x_1, x_2, Le_{CO}, Le_{H_2} are the volumetric fraction and Lewis number of signal-component fuel, respectively. Because the gas mixture is fuel-lean condition in current study, the final Lewis number is equal to the Lewis number of syngas.

The global turbulent burning velocity under different hydrogen fractions is shown in Fig. 9, where error bar is the standard deviation of five loops. And the original experimental data are also shown in Table 2. With turbulence intensity increased, global turbulent burning velocity is more sensitive to hydrogen fraction, as shown in Fig. 9 (a). Also, with hydrogen fraction increased, global turbulent burning velocity is more sensitive to turbulence intensity, as shown in Fig. 9 (b). According to the classical diffusional-thermal instability theory, as we all know, diffusional-thermal instability depends on two factors, the non-equal diffusion ability and the wrinkled degree of flamelets. The higher the turbulence intensity is, the more wrinkled the flamelets will become. And then the effects of diffusional-thermal instability will be strengthened, even if the non-equal diffusion ability is kept constant. Thus, global turbulent burning velocity will be more sensitive to the variation of hydrogen fraction at this time. Correspondingly, the higher the hydrogen fraction is, the more strengthened the non-equal diffusion will be. Then the diffusional-thermal instability will also be promoted. Thus, with strengthened non-equal diffusion ability, global turbulent burning velocity will be more sensitive to the wrinkled degree of flamelets, which depends on turbulence intensity.

Fig. 10 (a) is the normalized turbulent burning velocity S_T/S_L. Usually the effects of laminar burning velocity can be eliminated through this non-dimensional method. It is easy to understand that S_T/S_L is increased with turbulence intensity. However, with hydrogen fraction increased, S_T/S_L is nearly kept constant, and even has a slight decrease. Besides, this phenomenon is not limited to syngas/air flames, but also methane/hydrogen/air flames [30] and iso-octane/hydrogen/air flames [20], as long as equivalence ratio remains constant. Although the growth of turbulent burning velocity can be partially attributed to the growth of laminar burning velocity, other factors also have significant effects on this issue. It has been validated that keeping laminar burning velocity constant, in other words, the ratio of oxygen is reduced at this time, S_T/S_L will be increased with hydrogen fraction, just as the results of Muppala et al. [31]. In face of this seemingly contradictory phenomenon, it is necessary to give a more detailed and comprehensive interpretation here. We know that with hydrogen fraction increased, the effects of diffusional-thermal instability will be strengthened, which can promote S_T/S_L. However, our experimental results show that it is nearly kept constant, concluding that there should be other inhibiting factors. Except for laminar burning velocity and diffusional-thermal instability, a possible reason is the stretch effects of turbulence itself. Karlovitz number (Ka) stands for dimensionless stretch rate and can be evaluated by $Ka = \left(\frac{u'}{S_L}\right)^{3/2}\left(\frac{L_T}{\delta_L}\right)^{-1/2}$. As shown in Fig. 10 (b), Karlovitz number is decreased with hydrogen fraction, especially when turbulence intensity is high, this trend is more evident. Thus, it indicates that the stretch effects of turbulence itself are weakened at high hydrogen fraction. This prediction can also be validated in Fig. 10 (c). Here, $\sigma S_{T,R}$ is the flame propagation speed of turbulent expanding flames and S_F is the flame propagation speed of laminar condition. The effects of laminar burning velocity and flame intrinsic instability can be eliminated in this normalized way and only effects of turbulence itself is retained here. As we can see, $\sigma S_{T,R}/S_F$ is decreased with hydrogen fraction, and especially in intense turbulence, this distinction is more obvious. In this condition, although the strengthened diffusional-thermal instability can

Table 2 – Relative flame parameters and experimental data under different hydrogen fractions, T = 298 K, $\varphi = 0.7$ (S_L is calculated by Davis model [54], $\delta_L = \mu/(\rho \cdot S_L)$).

Fuel	P (bar)	u' (m/s)	L_T (mm)	Le	δ_L (mm)	S_L (cm/s)	S_T (cm/s)	S_T/S_L
$CO/H_2 = 80/20$	0.5	1.77	9.66	1.05	0.076	43.50	78.32	1.80
	1	1.77	9.66	1.05	0.044	37.60	87.63	2.33
	1.5	1.77	9.66	1.05	0.032	34.30	104.60	3.05
	2	1.77	9.66	1.05	0.026	31.90	111.67	3.50
	2.5	1.77	9.66	1.05	0.022	30.10	113.08	3.76
	3	1.77	9.66	1.05	0.019	28.70	115.38	4.02
	3.5	1.77	9.66	1.05	0.017	27.40	119.57	4.36
	5	1.77	9.66	1.05	0.013	24.64	127.74	5.18
	1	0.89	7.44	1.05	0.044	37.60	61.33	1.63
	1	2.66	11.25	1.05	0.044	37.60	117.77	3.13
	1	2.54	12.53	1.05	0.044	37.60	140.39	3.73
$CO/H_2 = 50/50$	1	0.89	7.44	0.95	0.029	59.94	100.50	1.68
	1	1.77	9.66	0.95	0.029	59.94	139.38	2.33
	1	2.66	11.25	0.95	0.029	59.94	177.57	2.96
	1	3.54	12.53	0.95	0.029	59.94	212.93	3.55
$CO/H_2 = 20/80$	1	0.89	7.44	0.73	0.021	87.57	138.29	1.58
	1	1.77	9.66	0.73	0.021	87.57	195.34	2.23
	1	2.66	11.25	0.73	0.021	87.57	242.95	2.77
	1	3.54	12.53	0.73	0.021	87.57	276.62	3.16

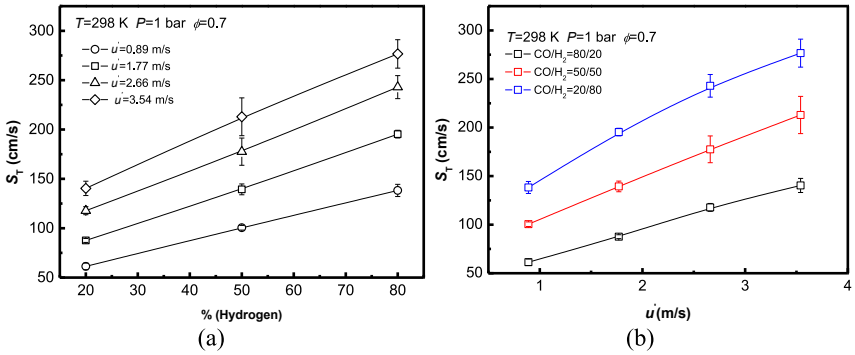

Fig. 9 – Global turbulent burning velocity under different hydrogen fractions: (a) x-axis is hydrogen fraction; (b) x-axis is u'.

promote turbulent burning velocity, the weakened stretch effects of turbulence will cause an opposite effect. And it is due to this trade off effect, S_T/S_L can be kept nearly constant with hydrogen fraction. When turbulence intensity is high, because the decline of turbulence stretch effects is more obvious, thus S_T/S_L even appears a slight decrease trend at this time. But when laminar burning velocity is kept constant, it means that the oxygen fraction must be reduced corresponding to the increase of hydrogen fraction. Compared to the fuel/air flames, the flame thickness will be increased when oxygen fraction is lower than 21%, resulting in a higher Karlovitz number. Although the stretch effects of turbulence are still weakened with hydrogen fraction, its weakened effects are not able to resist the strengthened thermal-diffusional instability any more. As a result, S_T/S_L is still increased with hydrogen fraction at this time. Therefore, it can be concluded that, the effects of hydrogen addition on turbulent burning velocity is the coupling results of laminar burning velocity, diffusional-thermal instability and turbulence stretch. But due to that strengthened diffusional-thermal instability and weakened turbulence stretch resist with each other, it seems that the growth of turbulent burning velocity only depends on laminar burning velocity.

Unified scaling of turbulent burning velocity

In order to derive a general correlation of turbulent burning velocity, a unified scaling has been conducted through dimensionless parameters. Turbulent burning velocity mainly depends on turbulence and laminar flame characteristics. Thus, these characteristics should be included as much as possible when conducting a unified scaling. Considering the definition of turbulent Reynolds number is

$$Re_T = u' L_T / \nu \tag{2}$$

where ν is kinematic viscosity, this dimensionless parameter can be used to reflect turbulence characteristics. At the same time, turbulent burning velocity is normalized by laminar burning velocity, to consider the effects of laminar flame characteristics.

Fig. 11 shows the unified scaling of global turbulent burning velocity. The experimental data can be collapsed into a line, suggesting that turbulent Reynolds number is a suitable method to correlate turbulent burning velocity. Qualitatively, S_T/S_L approximately follows power law with turbulent Reynolds number. And in quantitative level, current power exponent is 0.46, close to the experimental result 0.53 of Shy

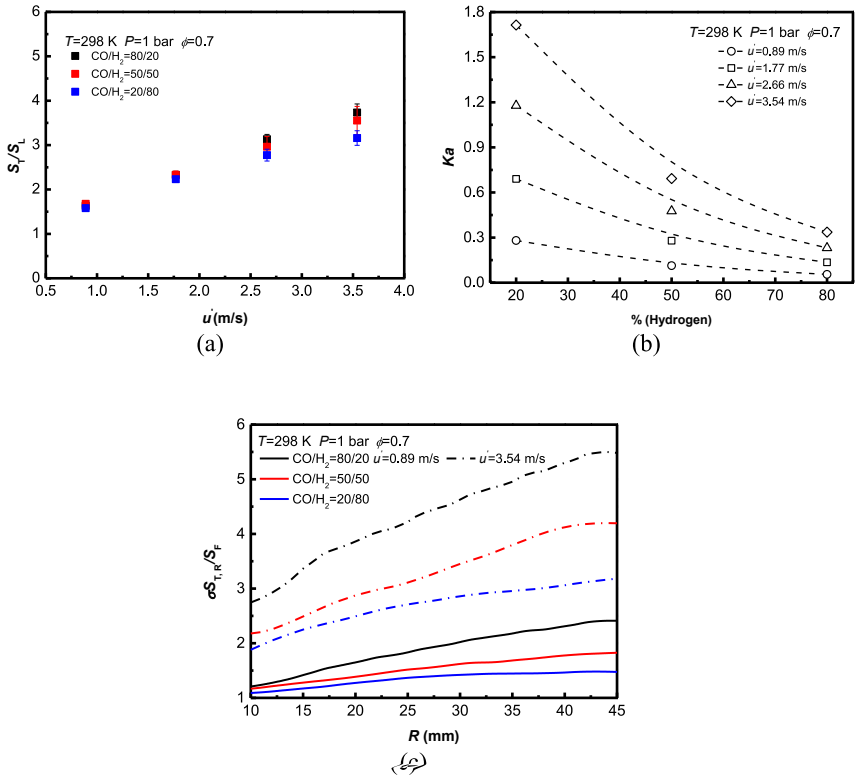

Fig. 10 – Normalized turbulent burning velocity and weakened turbulence stretch effects: (a) S_T/S_L; (b) Ka; (c) $\sigma S_{T,R}/S_F$.

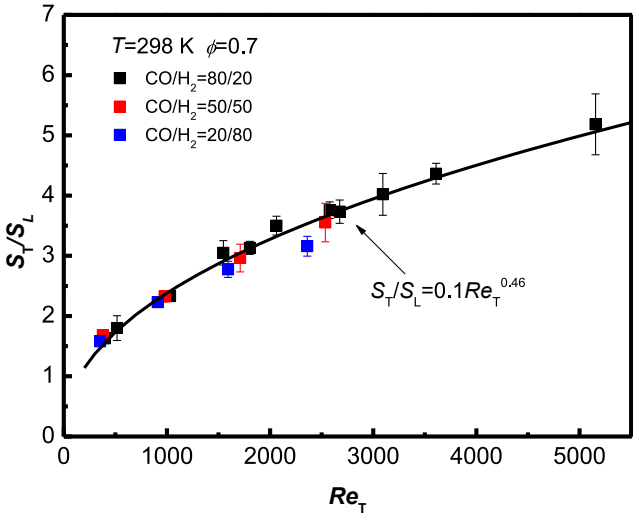

Fig. 11 – A unified scaling of global turbulent burning velocity through turbulent Reynolds number.

et al. [23] and theoretical result 0.5 of Chaudhuri et al. [41]. Thus, it validates that a satisfactory unified scaling can be obtained through turbulent Reynolds number again, and the quantitative relation is approximately $S_T/S_L \sim Re_T^{0.5}$, regardless of different turbulence intensities, initial pressures and fuels. It should be noted that, the current correlation is only applicable for $Le \approx 1$ conditions, because there is no parameter reflecting molecule transport in turbulent Reynolds number. However, this correlation gives a satisfactory performance for different hydrogen fraction conditions. This is mainly due to that most experimental conditions are about 20% hydrogen fraction, whose Lewis number is close to unity. In fact, even for 80% hydrogen fraction conditions, because equivalence ratio is 0.7 and not lean enough, Lewis number is about 0.73 (Table 2) at this time. Consider the inaccuracy of Lewis number estimation, it is still close to unity to some degree. Due to this, different hydrogen fraction conditions in current study can be correlated well with turbulent Reynolds number.

Different from turbulent stationary flames, the acceleration phenomenon is special and important for turbulent expanding flames, which usually leads to a large scatter of global turbulent burning velocity because the selected flame radius range is different between previous researches [23,26,46]. To eliminate this scatter, the acceleration phenomenon should be considered in unified scaling of turbulent burning velocity. According to previous researches, there are two approaches to reflect this acceleration, introducing effective turbulence intensity [45], or substituting integral length scale with flame radius [14]. And here, we will validate the capability of these two approaches respectively and combine them together to see if a better unified scaling can be achieved. Due to the satisfactory results of turbulent Reynolds number, the unified scaling here is also based on it. Thus, introducing effective turbulence intensity, flame radius and both of them, turbulent Reynolds number can be transferred to

$$Re_{T,eff} = u'_{eff} L_T / \nu \quad (3)$$

$$Re_f = u' R / \nu \quad (4)$$

$$Re_{f,eff} = u'_{eff} R / \nu \quad (5)$$

Here, they are named effective turbulent Reynolds number, flame Reynolds number and effective flame Reynolds number, respectively.

Besides, according to the turbulence characteristics estimation results [48], effective turbulence intensity is evaluated by

$$u'_{eff} = \left[\int_{\kappa_l}^{\kappa_c} E_{11}(\kappa) d\kappa \right]^{1/2} \quad (6)$$

Here, $E_{11}(\kappa)$ is turbulent kinetic energy density, the upper limitation κ_c is the cutoff wavenumber in spatial energy spectrum, and the lower limitation κ_l corresponds to the flame size and can be evaluated as $\kappa_l = \pi/R$. The results of effective turbulence intensity are shown in Fig. 12. Due to that turbulence intensity is not affected by initial pressure, here only the effects of fan frequency are investigated while the initial pressure is kept constant at 1.0 bar. In order to eliminate the effects of ignition and chamber confinement [49,50], the experimental radius domain of current chamber is 10–45 mm , thus the effective turbulence intensity is also estimated in this domain. From Fig. 12 (a), we can see that the higher effective turbulence intensity corresponds to a higher fan frequency under the same flame radius. With the flame propagating outwardly, the effective turbulence intensity will become larger continuously. The vortexes range which can wrinkle the flame will become wider with flame propagating and correspond to a larger turbulent kinetic energy, resulting in higher effective turbulence intensity. To consider the effects of fan frequency and flame radius, a general correlation of effective turbulence intensity has been obtained in Fig. 12 (b). The effective turbulence intensity collapses into a power law line very well under different fan frequency and flame radius, which indicates that the unification of the correlation is reasonable and can be used to estimate the effective turbulence intensity. It should be noted that the power law factor is 0.267, which is close to 0.23 of Chaudhuri [18] and 0.253 of Mannaa [55]. Such consistence indicates the reliability of current turbulence characteristics and a specific dependence between effective turbulence intensity and radius.

Fig. 13 is the unified scaling for transient turbulent burning velocity, corresponding to 20% hydrogen fraction condition. From Fig. 13 (a), we can see that although effective turbulence intensity is proposed to analyze and explain the acceleration phenomenon in turbulent expanding flames, there doesn't appear a satisfactory unified scaling through it. In other words, only effective turbulence intensity itself is not able to reflect the acceleration phenomenon. Oppositely, only substituting integral length scale with flame radius can achieve a reasonable unified scaling, as shown in Fig. 13 (b). Besides, an approximate power law appears between them, and the power exponent is 0.5. Similarly, when introducing both effective turbulence intensity and flame radius in Reynolds number, it can still give a satisfactory performance and appear a power law relationship, just as shown in Fig. 13 (c). To consider the acceleration phenomenon in unified scaling, a quantitative dependence between transient turbulent burning velocity and flame radius should be determined. Based on discussion above, it should be believed that this dependence is $S_{T,R}/S_L \sim R^{0.5}$ approximately. The effective turbulence intensity can be estimated by $u'_{eff} = 0.35 \cdot 10^{-3} \cdot \omega \cdot R^{0.267}$, meaning that the dependence between effective turbulence intensity and flame radius is $u'_{eff} \sim R^{0.267}$. Obviously, only effective turbulence intensity is not enough to reflect this acceleration quantitatively. In fact, when effective turbulence intensity and flame radius are introduced together, it can be derived that $S_{T,R}/S_L \sim (R^{0.267} \cdot R)^{0.45} \sim R^{0.57}$, which is still close to the square root of flame radius. Thus, no matter introducing flame radius itself or both flame radius and effective turbulence intensity, the final results are similar. We can conclude that, the turbulent expanding flames perform a self-similar propagation and the quantitative description of acceleration phenomenon in turbulent expanding flames is $S_{T,R}/S_L \sim R^{0.5}$approximately. The effective turbulence intensity is not able to reflect this acceleration completely, thus directly introducing flame radius is a suitable method in unified scaling of turbulent burning velocity, although integral length scale is neglected this way.

Through flame Reynolds number, a unified scaling of transient turbulent burning velocity for different hydrogen fractions is shown in Fig. 14. And the error bar is the standard deviation of five loops. As we can see, transient turbulent

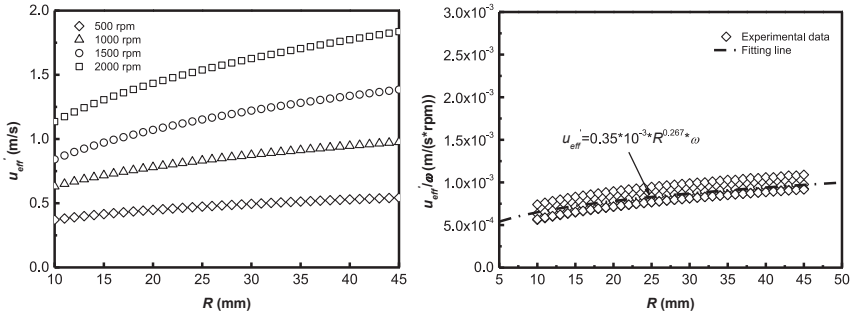

(a) (b)

Fig. 12 – Effective turbulence intensity: (a) under different conditions; (b) general correlation.

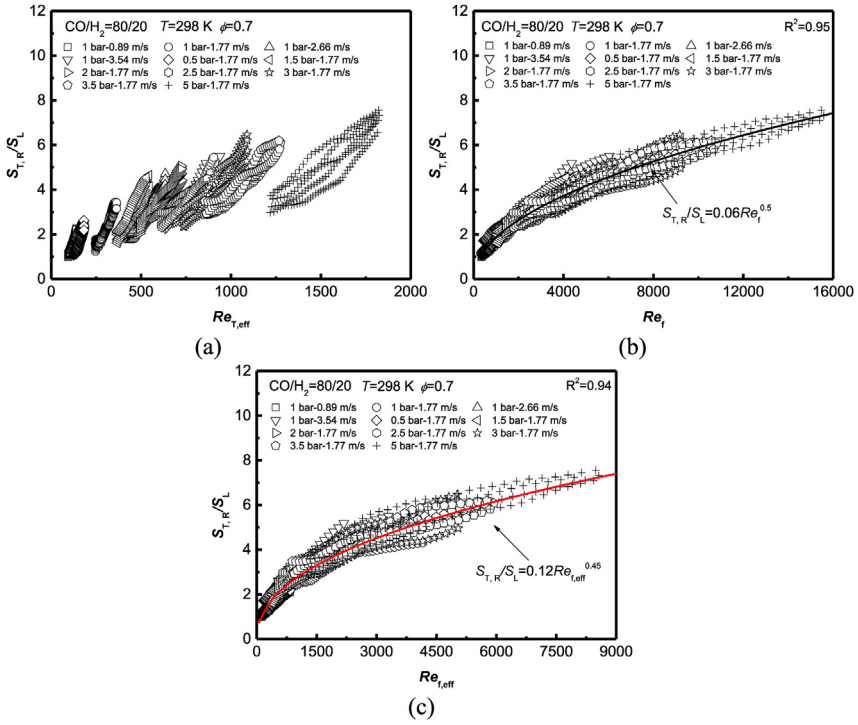

Fig. 13 – Unified scaling of transient turbulent burning velocity: (a) $Re_{T,\,eff}$; (b) Re_f; (c) $Re_{f,\,eff}$.

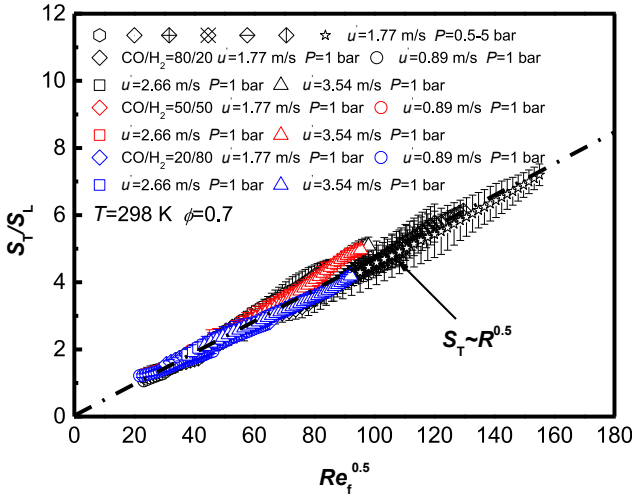

Fig. 14 – A unified scaling of transient turbulent burning velocity under different hydrogen fractions.

burning velocity of different hydrogen fractions can still be correlated by above approach. And $S_{T,R}/S_L \sim R^{0.5}$is still suitable at this time. However, it should be noted that, it doesn't mean the turbulent burning velocity of different molecule transport conditions can be scaled together through Reynolds number itself. Just as the discussions for global turbulent burning velocity, it is most likely that Lewis number of all gas mixtures is close to unity in current experiment, while for other $Le \neq 1$ conditions, such as different equivalence ratios and different single fuels, it will be invalid. In fact, without introduction of molecule transport parameters, it is almost impossible to extend this approach to $Le \neq 1$ conditions completely. Therefore, further study is needed to include the effects of molecule transport to obtain a robust general correlation.

Conclusions

Lean syngas/air turbulent expanding flames are investigated under different turbulence intensities (0–3.54 m/s), initial pressures (0.5–5 bar) and hydrogen fractions up to 80% (20%, 50% and 80%). The flame structure, turbulent burning velocity and its unified scaling are obtained and analyzed systematically.

The growth of turbulent burning velocity is caused by a larger flame surface area, while the latter is mainly dependent on turbulence stretch and flame intrinsic instability. With turbulence intensity and initial pressure increased, flame surface becomes more refined and wrinkled. Correspondingly, turbulent burning velocity is promoted as well, although the growth rate will gradually be slow at high pressure.

The effects of hydrogen addition on turbulent burning velocity are the coupling results of laminar burning velocity, diffusional-thermal instability and turbulence stretch. Under higher hydrogen fraction, turbulent burning velocity will be more sensitive to turbulence intensity. And under higher turbulence intensity, turbulent burning velocity will be more sensitive to hydrogen fraction as well. S_T/S_L is nearly kept constant with hydrogen fraction due to the trade-off effects between strengthened diffusional-thermal instability and weakened turbulence stretch.

Turbulent burning velocity can be unified scaling very well through turbulent Reynolds number, validating that it is indeed a practical correlation regardless of turbulence intensity and initial pressure. Turbulent expanding flames

follow a self-similar propagation law and the acceleration phenomenon can be described as $S_T/S_L \sim R^{0.5}$ approximately. Only effective turbulence intensity is not able to reflect the acceleration completely, while introducing flame radius into turbulent Reynolds number directly is a suitable method. The current general correlation is only applicable for $Le \approx 1$ conditions, and further study is needed to consider molecule transport effects.

Declaration of competing interest

The authors declare that they have no known competing financial interests or personal relationships that could have appeared to influence the work reported in this paper.

Acknowledgements

This study is supported by National Natural Science Foundation of China (No. 91841302, 51776164).

REFERENCES

[1] Huang Z, Zhang Y, Zeng K, Liu B, Wang Q, Jiang D. Measurements of laminar burning velocities for natural gas–hydrogen–air mixtures. Combust Flame 2006;146(1):302–11.
[2] Gnanapragasam N, Reddy B, Rosen M. Reducing CO2 emissions for an IGCC power generation system: effect of variations in gasifier and system operating conditions. Energy Convers Manag 2009;50(8):1915–23.
[3] Wright IG, Gibbons TB. Recent developments in gas turbine materials and technology and their implications for syngas firing. Int J Hydrogen Energy 2007;32(16):3610–21.
[4] Xie Y, Wang X, Bi H, Yuan Y, Wang J, Huang Z, Lei B. A comprehensive review on laminar spherically premixed flame propagation of syngas. Fuel Process Technol 2018;181:97–114.
[5] Okafor EC, Nagano Y, Kitagawa T. Experimental and theoretical analysis of cellular instability in lean H 2 -CH 4 -air flames at elevated pressures. Int J Hydrogen Energy 2016;41(15):6581–92.
[6] Sokolik AS, Karpov VP, Semenov ES. Turbulent combustion of gases 1967;3(1):36–45.
[7] Karpov VP, Severin ES. Effects of molecular-transport coefficients on the rate of turbulent combustion. Combust Explos Shock Waves 1980;16(1):41–6.
[8] Bradley D, Haq MZ, Hicks RA, Kitagawa T, Lawes M, Sheppard CGW, Woolley R. Turbulent burning velocity, burned gas distribution, and associated flame surface definition. Combust Flame 2003;133(4):415–30.
[9] Chaudhuri S, Wu F, Zhu D, Law CK. Flame speed and self-similar propagation of expanding turbulent premixed flames. Phys Rev Lett 2012;108(4):044503.
[10] Bradley D, Lau A, Lawes M, Smith F. Flame stretch rate as a determinant of turbulent burning velocity. Philos Trans R Soc London, Ser A: Physical and Engineering Sciences 1992;338(1650):359–87.
[11] Lawes M, Ormsby MP, Sheppard CGW, Woolley R. Variation of turbulent burning rate of methane, methanol, and Iiso-octane air mixtures with equivalence ratio at elevated pressure. Combust Sci Technol 2005;177(7):1273–89.
[12] Kitagawa T, Nakahara T, Maruyama K, Kado K, Hayakawa A, Kobayashi S. Turbulent burning velocity of hydrogen–air premixed propagating flames at elevated pressures. Int J Hydrogen Energy 2008;33(20):5842–9.
[13] Liu CC, Shy SS, Chiu CW, Peng MW, Chung HJ. Hydrogen/carbon monoxide syngas burning rates measurements in high-pressure quiescent and turbulent environment. Int J Hydrogen Energy 2011;36(14):8595–603.
[14] Swetaprovo C, Fujia W, Delin Z, Law CK. Flame speed and self-similar propagation of expanding turbulent premixed flames. Phys Rev Lett 2012;108(4):044503.
[15] Sun ZY, Li GX. Turbulence influence on explosion characteristics of stoichiometric and rich hydrogen/air mixtures in a spherical closed vessel. Energy Convers Manag 2017;149:526–35.
[16] Cai X, Wang J, Bian Z, Zhao H, Huang Z. Propagation of Darrieus–Landau unstable laminar and turbulent expanding flames. Proc Combust Inst 2021;38(2):2013–21.
[17] Goulier J, Comandini A, Halter F, Chaumeix N. Experimental study on turbulent expanding flames of lean hydrogen/air mixtures. Proc Combust Inst 2016;36(2).
[18] Chaudhuri S, Wu F, Law CK. Scaling of turbulent flame speed for expanding flames with Markstein diffusion considerations. Phys Rev 2013;88(3):033005.
[19] Sheng Yang AS, Liu Zirui, Law Chung K. Role of Darrieus-Landau instability in propagation of expanding turbulent flames. J Fluid Mech 2018;850:784–802.
[20] Fairweather M, Ormsby MP, Sheppard CGW, Woolley R. Turbulent burning rates of methane and methane-hydrogen mixtures. Combust Flame 2009;156(4):780–90.
[21] Bauwens CR, Bergthorson JM, Dorofeev SB. On the interaction of the Darrieus–Landau instability with weak initial turbulence. Proc Combust Inst 2017;36(2):2815–22.
[22] Liu CC, Shy SS, Chen HC, Peng MW. On interaction of centrally-ignited, outwardly-propagating premixed flames with fully-developed isotropic turbulence at elevated pressure. Proc Combust Inst 2011;33(1):1293–9.
[23] Liu CC, Shy SS, Peng MW, Chiu CW, Dong YC. High-pressure burning velocities measurements for centrally-ignited premixed methane/air flames interacting with intense near-isotropic turbulence at constant Reynolds numbers. Combust Flame 2012;159(8):2608–19.
[24] Chaudhuri S, Saha A, Law CK. On flame–turbulence interaction in constant-pressure expanding flames. Proc Combust Inst 2015;35(2):1331–9.
[25] Jiang LJ, Shy SS, Li WY, Huang HM, Nguyen MT. High-temperature, high-pressure burning velocities of expanding turbulent premixed flames and their comparison with Bunsen-type flames. Combust Flame 2016;172:173–82.
[26] Lawes M, Ormsby MP, Sheppard CGW, Woolley R. The turbulent burning velocity of iso-octane/air mixtures. Combust Flame 2012;159(5):1949–59.
[27] Brequigny P, Endouard C, Foucher F, Mounaïm-Rousselle C. Improvement of turbulent burning velocity measurements by schlieren technique, for high pressure isooctane-air premixed flames. Combust Sci Technol 2020;192(3).
[28] Bradley D, Lawes M, Mansour MS. Correlation of turbulent burning velocities of ethanol-air, measured in a fan-stirred bomb up to 1.2 MPa. Combust Flame 2011;158(1):123–38.
[29] Vancoillie J, Sharpe G, Lawes M, Verhelst S. The turbulent burning velocity of methanol–air mixtures. Fuel 2014;130:76–91.
[30] Mandilas C, Ormsby MP, Sheppard CGW, Woolley R. Effects of hydrogen addition on laminar and turbulent premixed methane and iso-octane–air flames. Proc Combust Inst 2007;31(1):1443–50.

[31] Muppala SPR, Nakahara M, Aluri NK, Kido H, Wen JX, Papalexandris MV. Experimental and analytical investigation of the turbulent burning velocity of two-component fuel mixtures of hydrogen, methane and propane. Int J Hydrogen Energy 2009;34(22):9258–65.
[32] Cai X, Wang J, Bian Z, Zhao H, Zhang M, Huang Z. Self-similar propagation and turbulent burning velocity of CH4/H2/air expanding flames: effect of Lewis number. Combust Flame 2020;212:1–12.
[33] Chiu C-W, Dong Y-C, Shy SS. High-pressure hydrogen/carbon monoxide syngas turbulent burning velocities measured at constant turbulent Reynolds numbers. Int J Hydrogen Energy 2012;37(14):10935–46.
[34] Jiang Y-h, Li G-x, Li H-m, Zhang G-p, Lv J-c. Study on the effect of hydrogen fraction on the premixed combustion characteristics of syngas/air mixtures. Energy 2020;200:117592.
[35] Zhang G-P, Li G-X, Li H-M, Jiang Y-H, Lv J-C. Experimental investigation on the self-acceleration of 10%H2/90%CO/air turbulent expanding premixed flame. Int J Hydrogen Energy 2019;44(44):24321–30.
[36] Sun Z, Xu C. Turbulent burning velocity of stoichiometric syngas flames with different hydrogen volumetric fractions upon constant-volume method with multi-zone model. Int J Hydrogen Energy 2020;45(7):4969–78.
[37] Sun ZY. Turbulent explosion characteristics of stoichiometric syngas. Int J Energy Res 2018;42(3):1225–36.
[38] D. V. a; L. V. b. Turbulent combustion modeling. Prog Energy Combust Sci 2002;28(3):193–266.
[39] Zimont VL. Gas premixed combustion at high turbulence. Turbulent flame closure combustion model. Experimental Thermal & Fluid Ence 2000;21(1–3):179–86.
[40] Peters N. The turbulent burning velocity for large-scale and small-scale turbulence. J Fluid Mech 1999;384(384):107–32.
[41] Chaudhuri S, V'Yacheslav A, Law CK. Spectral formulation of turbulent flame speed with consideration of hydrodynamic instability. Phys Rev 2011;84(2):026322.
[42] Kobayashi H, Kawabata Y, Maruta K. Experimental study on general correlation of turbulent burning velocity at high pressure. Symposium on Combustion 1998;27(1):941–8.
[43] Lipatnikov AN, Chomiak J. Turbulent flame speed and thickness: phenomenology, evaluation, and application in multi-dimensional simulations. Prog Energy Combust Sci 2002;28(1):1–74.
[44] Buckmaster J, Takeno T. Modeling in combustion science. 1995.
[45] Abdel-Gayed RG, Bradley D, Lawes M. Turbulent burning velocities: a general correlation in terms of straining rates. Proc Roy Soc Lond 1987;414(1847):389–413.
[46] Wu F, Saha A, Chaudhuri S, Law CK. Propagation speeds of expanding turbulent flames of C 4 to C 8 n -alkanes at elevated pressures: experimental determination, fuel similarity, and stretch-affected local extinction. Proc Combust Inst 2015;35(2):1501–8.
[47] Cai X, Wang J, Bian Z, Zhao H, Dai H, Huang Z. On transition to self-similar acceleration of spherically expanding flames with cellular instabilities. Combust Flame 2020;215:364–75.
[48] Zhao H, Wang J, Cai X, Bian Z, Dai H, Huang Z. Experimental study of turbulence characteristics and methanol/air spherically expanding flames. Frontiers in Energy accepted.
[49] Chen Z, Burke MP, Ju Y. Effects of Lewis number and ignition energy on the determination of laminar flame speed using propagating spherical flames. Proc Combust Inst 2009;32(1):1253–60.
[50] Burke MP, Chen Z, Ju Y, Dryer FL. Effect of cylindrical confinement on the determination of laminar flame speeds using outwardly propagating flames. Combust Flame 2009;156(4):771–9.
[51] Borghi R. On the structure and morphology of turbulent premixed flames. 1985.
[52] Renou B, Boukhalfa A, Puechberty D, Trinité M. Effects of stretch on the local structure of preely propagating premixed low-turbulent flames with various lewis numbers. Proc Combust Inst 1998;27(1):841–7.
[53] Lipatnikov AN, Chomiak J. Molecular transport effects on turbulent flame propagation and structure. Prog Energy Combust Sci 2004;31(1):1–73.
[54] Davis SG, Joshi AV, Hai W, Egolfopoulos F. An optimized kinetic model of H 2/CO combustion. Proc Combust Inst 2005;30(1):1283–92.
[55] Mannaa O, Brequigny P, Mounaim-Rousselle C, Foucher F, Chung SH, Roberts WL. Turbulent burning characteristics of FACE-C gasoline and TPRF blend associated with the same RON at elevated pressures. Exp Therm Fluid Sci 2018;95:104–14.